

Hartree–Fock orbital instability envelopes in highly correlated single-reference wave functions

T. Daniel Crawford

Center for Computational Quantum Chemistry, Department of Chemistry, The University of Georgia, Athens, Georgia 30602-2556, and Institute for Theoretical Chemistry, Departments of Chemistry and Biochemistry, The University of Texas, Austin, Texas 78712-1167

John F. Stanton

Institute for Theoretical Chemistry, Departments of Chemistry and Biochemistry, The University of Texas, Austin, Texas 78712-1167

Wesley D. Allen and Henry F. Schaefer III

Center for Computational Quantum Chemistry, Department of Chemistry, The University of Georgia, Athens, Georgia 30602-2556

(Received 18 August 1997; accepted 19 September 1997)

The effects of Hartree–Fock orbital instabilities on force constant predictions at both Hartree–Fock and correlated levels of theory are investigated. Due to the quadratic dependence of the second derivative of correlated energies on the orbital rotation parameters, anomalous force constant singularities enveloped by “instability volcanoes” are given by the single-reference correlation methods examined here. Infinite-order coupled-cluster methods are indeed affected by the reference instability, but over a rather small region of the potential surface, whereas perturbative triples corrections tend to widen the coupled-cluster volcano. Finite-order many-body perturbation theory yields very wide volcanoes, and corresponding predictions of vibrational spectra may be seriously compromised if the geometry of interest lies at all in the vicinity of an instability in the reference determinant. © 1997 American Institute of Physics. [S0021-9606(97)01348-2]

I. INTRODUCTION

Model electronic wave functions are frequently constructed such that they maintain selected spin and spatial symmetry characteristics of the exact wave function. However, these wave functions are not always energetically optimal, and relaxation of symmetry constraints sometimes leads to lower-energy solutions. In such cases, the symmetry-adapted wave function is said to exhibit a symmetry-breaking instability. Hartree–Fock wave functions provide the classic example of this behavior in the prediction of the potential energy curve for molecular hydrogen. At long bond distances, spin-restricted (RHF) and -unrestricted (UHF) determinants give qualitatively different results, with the latter providing an energetically correct dissociation asymptote at the expense of significant spin impurity. Symmetry-broken wave functions are often not beneficial or even acceptable,¹ however, and the question of whether to relax constraints in the presence of an instability was originally described by Löwdin as the “symmetry dilemma.”²

Electronic wave function instabilities were first analyzed in detail by Paldus and Čížek,^{3–7} who characterized multiple solutions of the Hartree–Fock equations in terms of the eigenvalues of a Hessian (\mathbf{H}^0) comprised of the second derivative of the energy with respect to molecular orbital rotations.^{8–11} If all eigenvalues of \mathbf{H}^0 are positive, the given Hartree–Fock wave function corresponds to a local (perhaps global) minimum on the orbital rotation surface, while a negative eigenvalue (λ_-) corresponds to a maximum. If the rotations defined by the eigenvector of λ_- involve pairs of orbitals belonging to different irreducible representations of

the point group of the nuclear framework, a lower-energy, spatial-symmetry-broken Hartree–Fock wave function exists. Under these circumstances, unconstrained computations will usually converge to the symmetry-broken solution due to variational collapse. For the determination of many molecular properties by finite difference procedures (e.g., force constants for non-symmetric vibrations), the existence of these symmetry-breaking instabilities presents a serious obstacle not only for Hartree–Fock theory, but also for correlated methods which use the Hartree–Fock determinant as a reference.⁹

Examples of the difficulties caused by spatial symmetry breaking in Hartree–Fock wave functions are abundant in the literature.^{9,12–20} One of the earliest was given by Jackels and Davidson¹³ in their work on the two lowest doublet states of nitrogen dioxide. They reported that non-orthogonal configuration interaction calculations are useful in the construction of a qualitatively correct pair of potential surfaces for the \tilde{X}^2A_1 and \tilde{A}^2B_2 states of NO_2 from symmetry-broken Hartree–Fock wave functions associated with competing valence bond structures. Later, Engelbrecht and Liu¹⁴ studied the lowest 3A_2 and 3B_2 states of CO_2 and found that high-level multi-configuration self-consistent field (MCSCF) calculations predict that the equilibrium structure for the latter state is of C_{2v} symmetry. However, lower-level spin-restricted open-shell Hartree–Fock (ROHF) wave functions erroneously predict a C_s structure due to a nearby instability. Engelbrecht and Liu explained this phenomenon in chemical terms as a competition among resonance, charge separation, and orbital-symmetry-constraint energies. Other representa-

tive examples include the σ and π formyloxyl (HCO_2) radicals,¹⁵ the allyl radical,^{21–23} the lithium and sodium superoxides (LiO_2 and NaO_2),^{9,24} the nitrate radical (NO_3),¹⁶ the O_4^+ ion,¹⁷ the hydrogen-peroxide radical cation,^{18,19} triplet excited states of glyoxal,^{25,26} and core-hole states of numerous ionized metal clusters.^{27–30}

The \tilde{C}^2A_2 state of NO_2 ²⁰ provides an unusual example of apparent artifactual *symmetry-constraining* effects on the nuclear framework. At the ROHF level of theory, the equilibrium geometry of the \tilde{C} state is predicted to be of C_{2v} symmetry, while high-level coupled-cluster analyses [based on UHF, quasi-restricted Hartree–Fock (QRHF),³¹ and Brueckner determinants^{16,32–34}] indicate that the minimum-energy structure should be of C_s symmetry due to a pseudo-Jahn–Teller distortion.¹² This behavior is opposite to the artifactual *symmetry-breaking* effects on the nuclear framework observed for many other systems, although the source of the problem is the same: a nearby orbital instability in the Hartree–Fock wave function. Furthermore, the apparently incorrect symmetry predictions given by ROHF wave functions for the \tilde{C} state of NO_2 continue even when the method is improved to the ROHF-based coupled-cluster singles and doubles level including a perturbational estimate of connected triples [CCSD(T)]. The errors are corrected only when the method is extended to include full triples (ROHF-CCSDT). The UHF-, QRHF-, and Brueckner-based coupled-cluster predictions, on the other hand, do not suffer from this instability in the pertinent region of the potential energy surface. As a result these methods consistently predict that the C_s structure is energetically optimum.²⁰

The chemical origins of electronic symmetry breaking can often be explained in valence-bond terms as a competition between orbital size effects and resonance interactions.^{9,14,15} In doublet instability problems,^{9,15–24} if a Hartree–Fock determinant is allowed to break symmetry, one of two valence-bond-like solutions will be obtained in which the singly occupied orbital is localized on one of two equivalent centers. Such a wave function may variationally incorporate energy lowering due to orbital size effects by allowing the doubly occupied orbital to be more (or less) diffuse than its singly occupied counterpart. However, in localizing the orbitals, the energy lowering due to the resonance interaction between the valence-bond structures is compromised. On the other hand, the symmetry-restricted determinant best recovers the stabilizing resonance interaction, but its inclusion of the orbital size effect is incomplete. One solution to this problem is to combine the symmetry-broken wave functions in a two-configuration treatment. Indeed, for all of the symmetry-breaking examples cited above, a properly designed multiconfiguration^{12–14} approach is capable of overcoming problems in the reference wave function. This traditional approach to symmetry-breaking solutions is often more expensive than single-reference counterparts, and, for many correlation methods such as coupled-cluster theory, are often poorly developed for general application. A second option lies in Brueckner-orbital methods,^{16,32–34} such as those based on the coupled-cluster

ansatz. Although Brueckner determinants are not *a priori* impervious to symmetry breaking,³⁵ they appear to have a propensity for preserving electronic symmetry.^{16–19,36,37} Some effort has been devoted to this area in recent years,^{37,38} and it is hoped that routine application of such methods to open-shell systems will eventually become more affordable.

This review makes it clear that in some cases even high levels of correlation may be unable to overcome inadequacies in the single-determinant reference wave function. However, certain important questions remain unanswered: What general behavior can be expected of force constants computed using correlated wave functions based on unstable reference determinants; and over what range of geometries will correlated wave functions be spuriously affected by reference instabilities? In this work we examine the effects of spatial-symmetry-breaking orbital instabilities on force constants obtained at both Hartree–Fock and single-reference correlated levels of theory. In Section III, we investigate the behavior of ROHF and UHF quadratic force constants for antisymmetric stretching in the ground state of LiO_2 . Anomalous Hartree–Fock-level force constants computed in regions of orbital instabilities have been investigated previously by Allen *et al.* for LiO_2 ⁹ and by Xie *et al.* for HOOH^+ ,¹⁸ and the relationship between such force constants and singularities in the molecular orbital Hessian has been discussed in detail by Burton, Yamaguchi, Alberts, and Schaefer.¹¹ Moreover, several other examples^{17,19} of unphysical theoretical vibrational frequencies engendered by symmetry-breaking phenomena have been reported but not subjected to a unified analysis. Such symmetry-breaking cases contrast those in which the potential surfaces of distinct physical states of different electronic symmetry intersect, a circumstance known for some time³⁸ to also produce singularities in the orbital response equations, as well as related vibrational frequencies and molecular properties, provided a connecting nuclear perturbation exists. Here we continue previous work by means of a general and unified analysis of the expression for the second derivative of the Hartree–Fock energy with respect to nuclear perturbations. In Section IV, we extend this analysis to finite-order many-body perturbation theory³⁹ and coupled-cluster methods,⁴⁰ all of which utilize the Hartree–Fock determinant as a reference wavefunction.

II. COMPUTATIONAL DETAILS

Quadratic force constants for antisymmetric stretching in \tilde{X}^2A_2 LiO_2 were computed at several levels of theory as a function of the O–O distance with the equivalent Li–O distances held fixed at the corresponding ROHF optimized value of 1.7887 Å. In order to avoid the difficulties associated with variational collapse in finite-difference procedures, all second derivative computations were carried out analytically at the ROHF, UHF, MBPT(2), MBPT(4), SDQ-MBPT(4), CCSD,^{31,41} CCSD+T(CCSD),⁴² and CCSD(T)^{43,44} levels of theory. The GAUSSIAN94 package was used to compute force constants at the MBPT(2) level, and a local version of the ACESII package^{45–47} was used at all oth-

ers. UHF wave functions were used as references for all correlated methods. The internal coordinates used were the O–O stretch and the symmetric and antisymmetric combinations of Li–O stretches. The force constants were computed by rigorous transformation of the Cartesian gradient and Hessian to internal coordinates using the INTDER95 program.^{48,49}

The basis set used on the oxygen atoms consisted of the standard Huzinaga–Dunning^{50,51} double-zeta set of contracted Gaussian functions with one additional set of higher-angular-momentum *d*-type polarization functions added.⁵² The contraction scheme for this basis is (9s5p1d/4s2p1d). Pure angular momentum functions were used for all *d*-type orbitals. The basis set used on the lithium atom was the double-zeta set of contracted functions given by Thakkar, Koga, Saito, and Hoffmeyer.⁵³ The contraction scheme for this basis is (9s5p/4s2p).

III. HARTREE–FOCK ANALYSIS

The Hartree–Fock electronic energy, E^0 , is a function of optimized orbital-rotation variables ($\boldsymbol{\kappa}$) and non-optimized parameters ($\boldsymbol{\rho}$), such as one- and two-electron integrals dependent on the atomic-orbital basis functions. Because the $\boldsymbol{\kappa}$ -gradient of E^0 always vanishes in this construction, the second derivative of $E^0(\boldsymbol{\kappa}, \boldsymbol{\rho})$ with respect to nuclear coordinates α and β may be written as

$$\frac{\partial^2 E^0}{\partial \alpha \partial \beta} = \sum_{ij} \left[\frac{\partial^2 E^0}{\partial \rho_i \partial \kappa_j} \left(\frac{\partial \kappa_j}{\partial \beta} \right) \left(\frac{\partial \rho_i}{\partial \alpha} \right) + \frac{\partial^2 E^0}{\partial \rho_i \partial \rho_j} \left(\frac{\partial \rho_j}{\partial \beta} \right) \times \left(\frac{\partial \rho_i}{\partial \alpha} \right) \right] + \sum_i \frac{\partial E^0}{\partial \rho_i} \left(\frac{\partial^2 \rho_i}{\partial \alpha \partial \beta} \right). \quad (1)$$

This equation may be converted to a convenient vector notation by defining

$$\begin{aligned} (\mathbf{H}_{\gamma\eta})_{ij} &\equiv \frac{\partial^2 E}{\partial \gamma_i \partial \eta_j}, & (\mathbf{g}_\gamma)_i &\equiv \frac{\partial E}{\partial \gamma_i}, \\ (\boldsymbol{\gamma}^\alpha)_i &\equiv \frac{\partial \gamma_i}{\partial \alpha}, & \text{and} & \quad (\boldsymbol{\gamma}^{\alpha\beta})_i &\equiv \frac{\partial^2 \gamma_i}{\partial \alpha \partial \beta}, \end{aligned}$$

where γ and η are used to denote general function variables or parameters, and superscripts will be used for \mathbf{H} and \mathbf{g} to denote the particular energy under differentiation. Hence,

$$\frac{\partial^2 E^0}{\partial \alpha \partial \beta} = (\boldsymbol{\rho}^\alpha)^\dagger \mathbf{H}_{\rho\kappa}^0 \boldsymbol{\kappa}^\beta + (\boldsymbol{\rho}^\alpha)^\dagger \mathbf{H}_{\rho\rho}^0 \boldsymbol{\rho}^\beta + (\mathbf{g}_\rho^0)^\dagger \boldsymbol{\rho}^{\alpha\beta}. \quad (2)$$

The molecular orbital rotation derivatives, $\boldsymbol{\kappa}^\beta$ of Eq. (2), may be computed *via* the first-order coupled-perturbed Hartree–Fock (CPHF) equations,⁵⁴ represented here as

$$\mathbf{H}_{\kappa\kappa}^0 \boldsymbol{\kappa}^\beta + \mathbf{H}_{\kappa\rho}^0 \boldsymbol{\rho}^\beta = 0, \quad (3)$$

where $\mathbf{H}_{\kappa\kappa}^0$ is the molecular orbital Hessian. Defining $\mathbf{B}_\kappa^\beta \equiv \mathbf{H}_{\kappa\rho}^0 \boldsymbol{\rho}^\beta$, $\boldsymbol{\kappa}^\beta$ is then given by

$$\boldsymbol{\kappa}^\beta = -(\mathbf{H}_{\kappa\kappa}^0)^{-1} \mathbf{B}_\kappa^\beta. \quad (4)$$

We may then apply a spectral decomposition⁵⁵ of $\mathbf{H}_{\kappa\kappa}^0$,

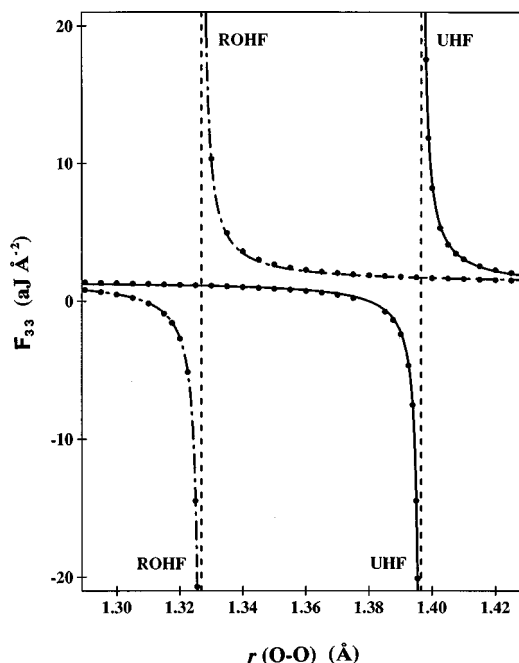


FIG. 1. Spin-restricted (ROHF) and -unrestricted (UHF) Hartree–Fock quadratic force constants (in $\text{aJ}/\text{\AA}^2$) for antisymmetric stretching in $\bar{X}^2 A_2$ LiO_2 as a function of the O–O distance (in \AA).

$$\mathbf{H}_{\kappa\kappa}^0 = \mathbf{V}_\kappa \boldsymbol{\Lambda}_\kappa \mathbf{V}_\kappa^\dagger, \quad (5)$$

where $\boldsymbol{\Lambda}_\kappa$ is a diagonal matrix containing the eigenvalues of $\mathbf{H}_{\kappa\kappa}^0$ and the columns of \mathbf{V}_κ are comprised of the corresponding eigenvectors. This decomposition gives for the orbital rotation parameters

$$\boldsymbol{\kappa}^\beta = -\mathbf{V}_\kappa \boldsymbol{\Lambda}_\kappa^{-1} \bar{\mathbf{B}}_\kappa^\beta, \quad (6)$$

where $\bar{\mathbf{B}}_\kappa^\beta \equiv \mathbf{V}_\kappa^\dagger \mathbf{B}_\kappa^\beta$. Inserting Eq. (6) into Eq. (2) gives the final expression for the second derivative of the Hartree–Fock energy,

$$\frac{\partial^2 E^0}{\partial \alpha \partial \beta} = -(\bar{\mathbf{B}}_\kappa^\alpha)^\dagger \boldsymbol{\Lambda}_\kappa^{-1} \bar{\mathbf{B}}_\kappa^\beta + (\boldsymbol{\rho}^\alpha)^\dagger \mathbf{H}_{\rho\rho}^0 \boldsymbol{\rho}^\beta + (\mathbf{g}_\rho^0)^\dagger \boldsymbol{\rho}^{\alpha\beta}. \quad (7)$$

As indicated earlier, the stability of a given solution of the Hartree–Fock equations may be characterized in terms of the eigenvalues, λ_i , of the molecular orbital Hessian. In regions of the potential energy surface where the competition between resonance and orbital-size effects is greatest, an eigenvalue, λ^* , of $\mathbf{H}_{\kappa\kappa}^0$ approaches zero; that is, the Hessian becomes singular. As a result, the first term on the right-hand side of Eq. (7) will dominate the expression for force constants within the same symmetry block as λ^* , and the associated harmonic vibrational frequencies will be anomalously large. Considering the diagonal, quadratic force constants only (i.e., $\alpha = \beta$), the overall sign of the force constant will be negative when λ^* is positive, indicating that the symmetry-constrained wave function is stable. However, when λ^* is negative, indicating that a symmetry-broken wave function is lower in energy, the force constant will be positive. In brief, a first-order pole in the force constant $F_{\alpha\alpha}$ appears at λ^* . This behavior is a consequence of the linear

dependence of the second derivative on the orbital rotation parameters, $\boldsymbol{\kappa}^\beta$, and would also be expected of multi-configuration self-consistent-field (MCSCF) wave functions.

In Figure 1, the Hartree–Fock quadratic force constants for antisymmetric stretching for C_{2v} -constrained 2A_2 LiO₂ are plotted as a function of the O–O distance. A singularity is observed at a $r(\text{O–O}) = 1.3267 \text{ \AA}$ for the ROHF wave function, and further out at $r(\text{O–O}) = 1.3965 \text{ \AA}$ for the UHF wave function. For both types of Hartree–Fock determinants, the behavior described above is clearly observed. As described in detail in Ref. 9, for smaller O–O distances, the lowest-energy solution to the Hartree–Fock equations is symmetry-constrained; the singly occupied orbital is delocalized across the equivalent oxygens. For longer O–O distances, however, two mirror-image solutions in which the unpaired electron is localized on one oxygen or the other are more stable,⁹ and a single negative eigenvalue of $\mathbf{H}_{\kappa\kappa}^0$ is encountered. Thus, in accordance with Eq. (7), when the singularity is approached from shorter O–O distances, the force constant decreases without bound, but when approached from longer distances, the force constant increases to positive infinity. The force constants corresponding to the totally symmetric vibrations are not affected by the Hartree–Fock instability since the singularity occurs only in the b_2 -symmetry block of the molecular orbital Hessian.

IV. CORRELATION ANALYSIS

The total electronic energy is a sum of the Hartree–Fock energy, E^0 , and the correlation energy, E' , which itself is a function of the molecular orbital rotations ($\boldsymbol{\kappa}$) and other parameters ($\boldsymbol{\omega}$) some of which may be optimized, such as configuration coefficients. The parameters $\boldsymbol{\rho}$ comprise a subset of $\boldsymbol{\omega}$. Using the notation defined in the previous section, the second derivative of the correlation energy is given by

$$\begin{aligned} \frac{\partial^2 E'}{\partial \alpha \partial \beta} = & (\boldsymbol{\kappa}^\alpha)^\dagger \mathbf{H}'_{\kappa\kappa} \boldsymbol{\kappa}^\beta + (\boldsymbol{\kappa}^\alpha)^\dagger \mathbf{H}'_{\kappa\omega} \boldsymbol{\omega}^\beta + (\mathbf{g}'_\kappa)^\dagger \boldsymbol{\kappa}^{\alpha\beta} \\ & + (\boldsymbol{\omega}^\alpha)^\dagger \mathbf{H}'_{\omega\kappa} \boldsymbol{\kappa}^\beta + (\boldsymbol{\omega}^\alpha)^\dagger \mathbf{H}'_{\omega\omega} \boldsymbol{\omega}^\beta + (\mathbf{g}'_\omega)^\dagger \boldsymbol{\omega}^{\alpha\beta}. \end{aligned} \quad (8)$$

The first-order orbital rotation derivatives, $\boldsymbol{\kappa}^\alpha$, may be determined via Eq. (6). The second-order counterparts, $\boldsymbol{\kappa}^{\alpha\beta}$, may be computed using the second-order CPHF equations,⁵⁴ represented here as

$$\mathbf{H}_{\kappa\kappa}^0 \boldsymbol{\kappa}^{\alpha\beta} = -\mathbf{B}_{\kappa}^{\alpha\beta}. \quad (9)$$

Component i of $\mathbf{B}_{\kappa}^{\alpha\beta}$ is given by

$$\begin{aligned} (\mathbf{B}_{\kappa}^{\alpha\beta})_i \equiv & [(\boldsymbol{\kappa}^\alpha)^\dagger \mathbf{H}_{\kappa\kappa}^{\kappa_i} \boldsymbol{\kappa}^\beta + (\boldsymbol{\kappa}^\alpha)^\dagger \mathbf{H}_{\kappa\rho}^{\kappa_i} \boldsymbol{\rho}^\beta + (\boldsymbol{\rho}^\alpha)^\dagger \mathbf{H}_{\rho\kappa}^{\kappa_i} \boldsymbol{\kappa}^\beta \\ & + (\boldsymbol{\rho}^\alpha)^\dagger \mathbf{H}_{\rho\rho}^{\kappa_i} \boldsymbol{\rho}^\beta + (\mathbf{H}_{\kappa\rho}^0 \boldsymbol{\rho}^{\alpha\beta})_i], \end{aligned} \quad (10)$$

where

$$(\mathbf{H}_{\gamma\eta}^{\kappa_i})_{jk} \equiv \frac{\partial^3 E^0}{\partial \kappa_i \partial \gamma_j \partial \eta_k}. \quad (11)$$

Using $\boldsymbol{\kappa}^{\alpha\beta} = -(\mathbf{H}_{\kappa\kappa}^0)^{-1} \mathbf{B}_{\kappa}^{\alpha\beta}$, the third term on the right-hand side of Eq. (8) becomes,

$$(\mathbf{g}'_\kappa)^\dagger \boldsymbol{\kappa}^{\alpha\beta} = -(\mathbf{g}'_\kappa)^\dagger (\mathbf{H}_{\kappa\kappa}^0)^{-1} \mathbf{B}_{\kappa}^{\alpha\beta} = -\mathbf{Z}_\kappa^\dagger \mathbf{B}_{\kappa}^{\alpha\beta}, \quad (12)$$

where the \mathbf{Z} -vector⁵⁶ is defined by

$$\mathbf{Z}_\kappa \equiv (\mathbf{H}_{\kappa\kappa}^0)^{-1} \mathbf{g}'_\kappa. \quad (13)$$

Inserting Eq. (13) into Eq. (8) gives

$$\begin{aligned} \frac{\partial^2 E'}{\partial \alpha \partial \beta} = & (\boldsymbol{\kappa}^\alpha)^\dagger \mathbf{H}'_{\kappa\kappa} \boldsymbol{\kappa}^\beta + (\boldsymbol{\kappa}^\alpha)^\dagger \mathbf{H}'_{\kappa\omega} \boldsymbol{\omega}^\beta - \mathbf{Z}_\kappa^\dagger \mathbf{B}_{\kappa}^{\alpha\beta} \\ & + (\boldsymbol{\omega}^\alpha)^\dagger \mathbf{H}'_{\omega\kappa} \boldsymbol{\kappa}^\beta + (\boldsymbol{\omega}^\alpha)^\dagger \mathbf{H}'_{\omega\omega} \boldsymbol{\omega}^\beta + (\mathbf{g}'_\omega)^\dagger \boldsymbol{\omega}^{\alpha\beta}. \end{aligned} \quad (14)$$

Application of the first-order CPHF equations given in Eq. (6) reveals that the first term on the right-hand side of Eq. (14) and the first term in the definition of $\mathbf{B}_{\kappa}^{\alpha\beta}$ given by Eq. (10) both depend quadratically on the inverse of the eigenvalues of the molecular orbital Hessian. All other terms in Eqs. (14) and (10) have at most a linear dependence. However, the \mathbf{Z} -vector itself also depends on Λ_κ^{-1} , as shown by insertion of Eq. (5) into Eq. (13),

$$\mathbf{Z}_\kappa = \mathbf{V}_\kappa \Lambda_\kappa^{-1} \mathbf{V}_\kappa^\dagger \mathbf{g}'_\kappa. \quad (15)$$

If the sum over the orbital rotation eigenvectors implied by Eq. (15) is separated into symmetric and non-symmetric rotations,

$$\mathbf{Z}_\kappa = \sum_\gamma \frac{\mathbf{v}_\gamma (\mathbf{v}_\gamma^\dagger \mathbf{g}'_\kappa)}{\lambda_\gamma} + \sum_\eta \frac{\mathbf{v}_\eta (\mathbf{v}_\eta^\dagger \mathbf{g}'_\kappa)}{\lambda_\eta}, \quad (16)$$

then only the symmetric components survive since the energy gradient for non-symmetric orbital rotations is zero, i.e., $\mathbf{v}_\eta^\dagger \mathbf{g}'_\kappa = 0$.⁵⁷ Therefore, in the case of a singularity in the molecular orbital Hessian resulting from the existence of a symmetry-breaking Hartree–Fock orbital instability, \mathbf{Z}_κ will be unaffected, i.e., it will have no poles. Only those terms in Eqs. (14) and (10) involving the first-order orbital rotation derivatives, $\boldsymbol{\kappa}^\alpha$, will be influenced by the singularity. As a result, the second derivative of the correlation energy depends at most quadratically on the non-symmetric components of Λ_κ^{-1} . As the molecular geometry approaches the region of the potential energy surface in which a symmetry-breaking orbital instability exists, these quadratic terms will dominate the force constant expression, and the associated harmonic vibrational frequencies within the same symmetry block as the singularity will be anomalously large. However, unlike the Hartree–Fock force constants, which depend only linearly on the orbital rotation derivatives, $\boldsymbol{\kappa}^\alpha$, the correlated-level force constants approach either positive or negative infinity, but with the same sign on both sides of the singularity because the pole is second order. Furthermore, this quadratic dependence suggests that as the singularity is approached, the correlated-level force constants will blow up more rapidly than their Hartree–Fock counterparts. This behavior leads to a correlated ‘‘instability volcano.’’ The overall sign of the force constant curves will depend on the signs and relative magnitudes of \mathbf{Z}_κ , $\mathbf{H}'_{\kappa\kappa}$ and $\mathbf{H}_{\kappa\kappa}^0$, which multiply the quadratic Λ_κ^{-1} terms, and cannot be deduced *a priori*.

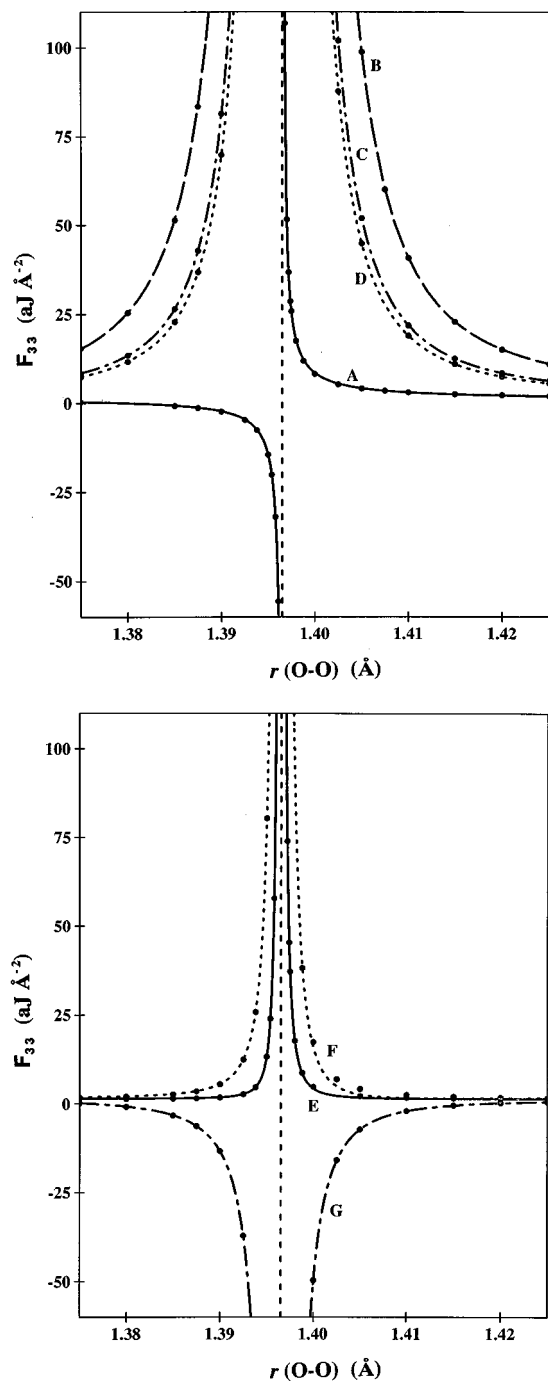


FIG. 2. Finite-order many-body perturbation theory (top) and coupled-cluster (bottom) quadratic force constants (in $\text{aJ}/\text{\AA}^2$) for antisymmetric stretching in \bar{X}^2A_2 LiO_2 as a function of the O–O distance (in \AA) in the region of the UHF reference wave function instability: (A) UHF; (B) MBPT(2); (C) MBPT(4); (D) SDQ-MBPT(4); (E) CCSD; (F) CCSD(T); (G) CCSD+T(CCSD).

For each of the correlated methods described in Section II, the quadratic force constant for antisymmetric stretching in LiO_2 is plotted in Figure 2 as a function of the O–O distance near the UHF instability discussed in section III. The values plotted in the figure are given in Table I. The width of each instability volcano provides some measure of the sensitivity of each method to the choice of reference

function, and therefore the associated capacity to overcome problems in describing the competing resonance and orbital-size effects. Clearly the poorest predictions are given by the three finite-order perturbation theory methods. MBPT(2) gives an exceptionally wide volcano, indicating that its quadratic force constant predictions are affected by the reference instability over a larger range of geometries than those of the UHF wave function itself. While the SDQ-MBPT(4) predictions offer an improvement over MBPT(2), inclusion of triple excitation terms to give full MBPT(4) slightly widens the volcano.

For the coupled-cluster methods, the best results are given by CCSD, which is affected by the reference instability over a rather narrow range of O–O bond lengths (less than 0.01\AA). However, inclusion of connected triple excitations *via* perturbation-based corrections serves to widen the volcano, as was also observed for MBPT. The CCSD(T) volcano is nearly 0.01\AA wider at its base than its CCSD counterpart, while the CCSD+T(CCSD) volcano is approximately 0.02\AA wider, but with the opposite sign of that given by all the other correlated methods. It is likely that if the coupled-cluster approaches were extended to the full CCSDT level (that is, including all triple excitations) the width of the instability volcano would be smaller than that found at the CCSD level. However, it is clear that the popular (T) correction, which is designed to serve as an approximation to CCSDT, is not an improvement over CCSD for symmetry-breaking cases such as LiO_2 .

V. CONCLUSIONS

We have investigated the effects of Hartree–Fock orbital instabilities on quadratic force constant predictions at both Hartree–Fock and correlated levels of theory. We have shown that, because of the quadratic dependence of the second derivative of the correlated energy on the orbital rotation parameters, force constant “instability volcanoes” are predicted by MBPT and coupled-cluster methods. This behavior differs qualitatively from that at the Hartree–Fock level where, due to the linear dependence of the second derivative of the energy on the orbital response, the force constants are shown to have opposite signs on either side of the singularity. Infinite-order coupled-cluster methods are affected by the reference instability over a rather small region of the potential surface, though perturbative corrections, such as the popular (T) correction, tend to widen the CCSD volcano. Finite-order MBPT methods produce very wide volcanoes and may be seriously affected in general if the geometry of interest lies at all in the vicinity of an instability in the reference determinant. The mathematical analysis presented here also applies fully to molecular properties such as polarizabilities, nuclear magnetic shielding tensors, and infrared intensities which involve analytic second derivatives of the energy with respect to external fields, magnetic moments, or nuclear perturbations. Moreover, the equations of Section III and IV can be readily extended to third- and higher-order derivatives, revealing relationships between the type and order of the force constants and the degree of the associated

TABLE I. UHF and UHF-based CC and MBPT quadratic force constants (in $\text{aJ}/\text{\AA}^2$) for anti-symmetric stretching in \bar{X}^2A_2 LiO_2 as a function of the O-O distance (in \AA).^a

$r(\text{O-O})$	UHF	MBPT(2)	SDQ-MBPT(4)	MBPT(4)	CCSD	CCSD+T(CCSD)	CCSD(T)
1.2700	1.4622	0.1888	1.8869	1.9197	1.7580	1.7771	1.7390
1.2750	1.4390	0.3449	1.8835	1.9189	1.7436	1.7629	1.7212
1.2800	1.4156	0.4992	1.8830	1.9203	1.7281	1.7492	1.7035
1.2850	1.3914	0.6528	1.8837	1.9241	1.7131	1.7354	1.6849
1.2900	1.3666	0.8070	1.8876	1.9314	1.6986	1.7221	1.6671
1.2950	1.3410	0.9634	1.8946	1.9417	1.6831	1.7096	1.6481
1.3000	1.3143	1.1235	1.9049	1.9574	1.6686	1.6967	1.6286
1.3050	1.2866	1.2895	1.9197	1.9781	1.6540	1.6846	1.6068
1.3100	1.2574	1.4644	1.9413	2.0057	1.6402	1.6722	1.5848
1.3150	1.2262	1.6519	1.9684	2.0411	1.6266	1.6610	1.5606
1.3200	1.1935	1.8566	2.0064	2.0865	1.6115	1.6497	1.5355
1.3250	1.1577	2.0852	2.0544	2.1478	1.5972	1.6406	1.5065
1.3300	1.1189	2.3469	2.1207	2.2243	1.5828	1.6309	1.4750
1.3350	1.0762	2.6543	2.2050	2.3281	1.5677	1.6235	1.4373
1.3400	1.0284	3.0262	2.3191	2.4658	1.5540	1.6164	1.3941
1.3450	0.9742	3.4909	2.4740	2.6513	1.5386	1.6139	1.3415
1.3500	0.9110	4.0927	2.6892	2.9065	1.5231	1.6124	1.2744
1.3550	0.8356	4.9046	2.9951	3.2685	1.5055	1.6178	1.1879
1.3600	0.7436	6.0523	3.4480	3.8004	1.4905	1.6303	1.0687
1.3650	0.6267	7.7706	4.1448	4.6208	1.4728	1.6546	0.8929
1.3700	0.4703	10.5357	5.2950	5.9713	1.4583	1.7067	0.6186
1.3750	0.2472	15.4412	7.3712	8.4036	1.4484	1.8149	0.1443
1.3850	-0.7466	51.4075	22.8992	26.5516	1.4825	2.7096	-3.2525
1.3875	-1.3306	83.4003	36.8010	42.8002	1.5614	3.5374	-6.2326
1.3900	-2.3579	159.2328	69.8320	81.4029	1.7897	5.5367	-13.2410
1.3925	-4.6540	—	183.3091	—	2.7227	12.4597	-37.0919
1.3938	-7.5097	—	—	—	4.6907	25.8146	-82.5734
1.3950	-14.4696	—	—	—	13.2059	80.3796	—
1.3954	-20.1004	—	—	—	23.9496	147.2901	—
1.3958	-31.9576	—	—	—	57.8693	—	—
1.3961	-55.5991	—	—	—	171.1650	—	—
1.3962	-73.2542	—	—	—	—	—	—
1.3963	-106.8104	—	—	—	—	—	—
1.3964	-195.2657	—	—	—	—	—	—
1.3965	—	—	—	—	—	—	—
1.3966	—	—	—	—	—	—	—
1.3968	106.8160	—	—	—	—	—	—
1.3970	51.6079	—	—	—	144.9695	—	—
1.3972	36.7625	—	—	—	73.9898	—	—
1.3974	28.6850	—	—	—	45.4301	—	—
1.3975	25.8837	—	—	—	37.1798	198.0813	—
1.3988	11.8538	—	—	—	8.7361	38.1957	-117.7660
1.4000	8.2124	—	—	—	4.8544	17.4207	-49.6416
1.4050	4.1244	98.8000	44.8363	51.9807	2.2086	4.2754	-7.0861
1.4100	3.0598	40.7858	19.0194	21.8898	1.8136	2.6089	-1.9120
1.4150	2.5657	22.8963	11.0121	12.5677	1.6668	2.0787	-0.3374
1.4200	2.2761	15.1169	7.5018	8.4846	1.5900	1.8388	0.3358
1.4250	2.0844	11.0468	5.6485	6.3322	1.5406	1.7051	0.6808
1.4300	1.9457	8.6554	4.5470	5.0528	1.5053	1.6204	0.8785
1.4350	1.8404	7.1347	3.8376	4.2310	1.4776	1.5617	1.0002
1.4400	1.7556	6.1113	3.3517	3.6690	1.4549	1.5180	1.0792
1.4450	1.6857	5.3938	3.0050	3.2680	1.4351	1.4835	1.1319
1.4500	1.6266	4.8757	2.7494	2.9728	1.4176	1.4554	1.1677
1.4550	1.5743	4.4949	2.5557	2.7504	1.4016	1.4315	1.1922
1.4600	1.5283	4.2139	2.4081	2.5808	1.3868	1.4104	1.2090
1.4650	1.4860	4.0102	2.2952	2.4523	1.3728	1.3915	1.2197
1.4700	1.4470	3.8723	2.2110	2.3580	1.3594	1.3743	1.2257

^aMissing entries signify anomalously large force constants which were determined to have an absolute value $> 200 \text{ aJ}/\text{\AA}^2$.

singularity. For example, the nonzero cubic force constants F_{33i} of LiO_2 should display second- and third-order poles, respectively, at the Hartree–Fock and correlated levels of theory. Thus, the profiles of the corresponding F_{33i} versus $r(\text{O}–\text{O})$ plots should be reversed relative to those displayed in Figure 2.

An important question addressed by this research relates to diagnostics which may be used to identify suspicious MBPT or coupled-cluster predictions of molecular properties due to nearby reference instabilities. Though no simple options exist at present, one approach is to monitor the magnitudes of the eigenvalues of the molecular orbital Hessian,^{10,11} since these will serve as a measure of the proximity of the current geometry to the point of singularity. Another effective alternative is to use coupled-cluster methods based on several types of reference wave functions (e.g., UHF, ROHF, QRHF or Brueckner determinants). CCSD and CCSD(T) results are generally expected to be approximately invariant to the choice of reference wave function when the system under investigation is well-behaved,⁵⁸ and strong deviations between UHF- and ROHF-CCSD predictions, for example, should be treated with caution.

ACKNOWLEDGMENTS

This research was sponsored by the National Science Foundation under Grant No. CHE-9527468. The authors thank Professors Jürgen Gauss and Peter Szalay for helpful discussions and for their work on the MBPT and CC analytic second derivative program which was essential to this research.

¹O. Goscinski, *Int. J. Quantum Chem. Symp.* **19**, 51 (1986).

²P. O. Löwdin, *Rev. Mod. Phys.* **35**, 496 (1963).

³J. Čížek and J. Paldus, *J. Chem. Phys.* **47**, 3976 (1967).

⁴J. Paldus and J. Čížek, *Chem. Phys. Lett.* **3**, 1 (1969).

⁵J. Paldus and J. Čížek, *J. Chem. Phys.* **52**, 2919 (1970).

⁶J. Paldus and J. Čížek, *J. Chem. Phys.* **54**, 2293 (1971).

⁷J. Paldus and J. Čížek, *Can. J. Chem.* **63**, 1803 (1985).

⁸K. Deguchi, K. Nishikawa, and S. Aono, *J. Chem. Phys.* **75**, 4165 (1981).

⁹W. D. Allen, D. A. Horner, R. L. DeKock, R. B. Remington, and H. F. Schaefer, *Chem. Phys.* **133**, 11 (1989).

¹⁰Y. Yamaguchi, I. L. Alberts, J. D. Goddard, and H. F. Schaefer, *Chem. Phys.* **147**, 309 (1990).

¹¹N. A. Burton, Y. Yamaguchi, I. L. Alberts, and H. F. Schaefer, *J. Chem. Phys.* **95**, 7466 (1991).

¹²E. R. Davidson and W. T. Borden, *J. Phys. Chem.* **87**, 4783 (1983).

¹³C. F. Jackels and E. R. Davidson, *J. Chem. Phys.* **64**, 2908 (1976).

¹⁴L. Engelbrecht and B. Liu, *J. Chem. Phys.* **78**, 3097 (1983).

¹⁵A. D. McLean, B. H. Lengsfeld, J. Pacansky, and Y. Ellinger, *J. Chem. Phys.* **83**, 3567 (1985).

¹⁶J. F. Stanton, J. Gauss, and R. J. Bartlett, *J. Chem. Phys.* **97**, 5554 (1992).

¹⁷L. A. Barnes and R. Lindh, *Chem. Phys. Lett.* **223**, 207 (1994).

¹⁸Y. Xie, W. D. Allen, Y. Yamaguchi, and H. F. Schaefer, *J. Chem. Phys.* **104**, 7615 (1996).

¹⁹J. Hrušák and S. Iwata, *J. Chem. Phys.* **106**, 4877 (1997).

²⁰T. D. Crawford, J. F. Stanton, P. G. Szalay, and H. F. Schaefer, *J. Chem. Phys.* **107**, 2525 (1997).

²¹D. B. Cook, *J. Chem. Soc. Faraday Trans.* **82**, 187 (1986).

²²J. Paldus and A. Veillard, *Mol. Phys.* **35**, 445 (1978).

²³P. G. Szalay, A. G. Császár, G. Fogarasi, A. Karpfen, and H. Lischka, *J. Chem. Phys.* **93**, 1246 (1990).

²⁴D. A. Horner, W. D. Allen, A. G. Császár, and H. F. Schaefer, *Chem. Phys. Lett.* **186**, 346 (1991).

²⁵E. R. Davidson and L. E. McMurchie, in *Excited States*, edited by E. C. Lim (Academic, New York, 1982), Vol. 5, pp. 1–39.

²⁶J. F. Gaw and H. F. Schaefer, *J. Chem. Phys.* **83**, 1741 (1985).

²⁷P. A. Cox, M. Bénard, and A. Veillard, *Chem. Phys. Lett.* **87**, 159 (1982).

²⁸M. Bénard, *Theor. Chim. Acta* **61**, 379 (1982).

²⁹M. D. Newton, *Chem. Phys. Lett.* **90**, 291 (1982).

³⁰M. Bénard, *Chem. Phys. Lett.* **96**, 183 (1983).

³¹M. Rittby and R. J. Bartlett, *J. Phys. Chem.* **92**, 3033 (1988).

³²R. K. Nesbet, *Phys. Rev.* **109**, 1632 (1958).

³³R. A. Chiles and C. E. Dykstra, *J. Chem. Phys.* **74**, 4544 (1981).

³⁴N. C. Handy, J. A. Pople, M. Head-Gordon, K. Raghavachari, and G. W. Trucks, *Chem. Phys. Lett.* **164**, 185 (1989).

³⁵J. Paldus, J. Čížek, and B. A. Keating, *Phys. Rev. A* **8**, 640 (1973).

³⁶T. J. Lee, R. Kobayashi, N. C. Handy, and R. D. Amos, *J. Chem. Phys.* **96**, 8931 (1992).

³⁷T. D. Crawford, T. J. Lee, N. C. Handy, and H. F. Schaefer, *J. Chem. Phys.* (in press); C. Hampel, K. A. Peterson, and H.-J. Werner, *Chem. Phys. Lett.* **190**, 1 (1992).

³⁸N. C. Handy, T. J. Lee, and W. H. Miller, *Chem. Phys. Lett.* **125**, 12 (1986).

³⁹R. J. Bartlett, *Annu. Rev. Phys. Chem.* **32**, 359 (1981).

⁴⁰R. J. Bartlett, in *Modern Electronic Structure Theory*, No. 2 in *Advanced Series in Physical Chemistry*, edited by D. R. Yarkony (World Scientific, Singapore, 1995), Chap. 16, p. 1047.

⁴¹G. D. Purvis and R. J. Bartlett, *J. Chem. Phys.* **76**, 1910 (1982).

⁴²M. Urban, J. Noga, S. J. Cole, and R. J. Bartlett, *J. Chem. Phys.* **83**, 4041 (1985).

⁴³K. Raghavachari, G. W. Trucks, J. A. Pople, and M. Head-Gordon, *Chem. Phys. Lett.* **157**, 479 (1989).

⁴⁴R. J. Bartlett, J. D. Watts, S. A. Kucharski, and J. Noga, *Chem. Phys. Lett.* **165**, 513 (1990), erratum: **167**, 609 (1990).

⁴⁵J. Gauss and J. F. Stanton, *Chem. Phys. Lett.* **276**, 70 (1997).

⁴⁶P. G. Szalay, J. Gauss, and J. F. Stanton (in preparation).

⁴⁷J. F. Stanton, J. Gauss, W. J. Lauderdale, J. D. Watts, and R. J. Bartlett, ACES II. The package also contains modified versions of the MOLECULE Gaussian integral program of J. Almlöf and P. R. Taylor, the ABACUS integral derivative program written by T. U. Helgaker, H. J. Aa. Jensen, P. Jørgensen and P. R. Taylor, and the PROPS property evaluation integral code of P. R. Taylor.

⁴⁸INTDER95 is a general program developed by Wesley D. Allen and co-workers which performs various vibrational analyses and higher-order nonlinear transformations among force field representations.

⁴⁹W. D. Allen and A. G. Császár, *J. Chem. Phys.* **98**, 2983 (1993).

⁵⁰S. Huzinaga, *J. Chem. Phys.* **42**, 1293 (1965).

⁵¹T. H. Dunning, *J. Chem. Phys.* **53**, 2823 (1970).

⁵²The polarization exponent used with d -type functions in the oxygen basis was $\alpha_d(\text{O})=1.211$, as optimized by L. T. Redmon, G. D. Purvis, and R. J. Bartlett, [*J. Am. Chem. Soc.* **101**, 285 (1979)].

⁵³A. J. Thakkar, T. Koga, M. Saito, and R. E. Hoffmeyer, *Int. J. Quantum Chem. Symp.* **27**, 343 (1993).

⁵⁴Y. Yamaguchi, Y. Osamura, J. D. Goddard, and H. F. Schaefer, *A New Dimension to Quantum Chemistry: Analytic Derivative Methods in Ab Initio Molecular Electronic Structure Theory*, No. 29 in *International Series of Monographs on Chemistry* (Oxford University Press, New York, 1994).

⁵⁵B. N. Parlett, *The Symmetric Eigenvalue Problem* (Prentice-Hall, Englewood Cliffs, 1980).

⁵⁶N. C. Handy and H. F. Schaefer, *J. Chem. Phys.* **81**, 5031 (1984).

⁵⁷We exclude from consideration here cases in which the molecular framework displays no symmetry (C_1) where \mathbf{g}'_{κ} has no vanishing components which are dictated by symmetry.

⁵⁸E. A. Salter, H. Sekino, and R. J. Bartlett, *J. Chem. Phys.* **87**, 502 (1987).